Wind and Structures, *Vol. 28, No. 4 (2019) 215-224*
DOI: https://doi.org/10.12989/was.2019.28.4.215

Experimental research on design wind loads of a large air-cooling structure

Xu Yazhou[1a], Ren Qianqian[*1], Bai Guoliang[1b] and Li Hongxing[2c]

[1]*School of Civil Engineering, Xi'an University of Architecture and Technology, Shaanxi, 710055, China*
[2]*Northwest Electric Power Design Institute, Shaanxi, 710075, China*

(Received February 8, 2018, Revised October 26, 2018, Accepted November 3, 2018)

Abstract. Because of the particularity and complexity of direct air-cooling structures (ACS), wind parameters given in the general load codes are not suitable for the wind-resistant design. In order to investigate the wind loads of ACS, two 1/150 scaled three-span models were designed and fabricated, corresponding to a rigid model and an aero-elastic model, and wind tunnel tests were then carried out. The model used for testing the wind pressure distribution of the ACS was defined as the rigid model in this paper, and the stiffness of which was higher than that of the aero-elastic model. By testing the rigid model, the wind pressure distribution of the ACS model was studied, the shape coefficients of "A" shaped frame and windbreak walls, and the gust factor of the windbreak walls were determined. Through testing the aero-elastic model, the wind-induced dynamic responses of the ACS model was studied, and the wind vibration coefficients of ACS were determined based on the experimental displacement responses. The factors including wind direction angle and rotation of fan were taken into account in this test. The results indicated that the influence of running fans could be ignored in the structural design of ACS, and the wind direction angle had a certain effect on the parameters. Moreover, the shielding effect of windbreak walls induced that wind loads of the "A" shaped frame were all suction. Subsequently, based on the design formula of wind loads in accordance with the Chinese load code, the corresponding parameters were presented as a reference for wind-resistant design and wind load calculation of air-cooling structures.

Keywords: direct air-cooling system; wind tunnel test; shape coefficient; wind vibration coefficient; wind load

1. Introduction

Taking advantage of water conservation, direct air-cooled condenser (ACC) is becoming more widespread in thermal power plants (Owen and Kröger 2011, Li *et al.* 2018, Butler and Grimes 2014). Since exhaust steam from a turbine is cooled by the ambient air in a closed loop system, there is no water evaporation compared to the traditional wet cooling technique. Particularly, in regions which are rich in coal while lacking of water, ACC is often a more attractive or even exclusive solution for large thermal power plants in order to saving water resources (He *et al.* 2013, Moore *et al.* 2014). Nevertheless, the direct air-cooled condenser in ACC takes the surrounding air as the cooling medium, which means that the ambient conditions such as wind and atmospheric instabilities have a great influence on the efficiency and normal operation of ACC systems (Maniscalco 2014, Chen *et al.* 2016, Yang *et al.* 2012). An air-cooling structure (ACS) generally consists of concrete tubular columns, steel platform, A-shaped frame and windbreak walls, as shown in Fig. 1. For the sake of cooling efficiency, ACC condensers are often installed on the steel platform with height of more than 40 m, it means that this kind of ACC structures must be a wind-sensitive structure. Additionally, it is well documented that ambient wind has a negative effect on the performance of ACC, i.e., reducing fan performance and hot plume recirculation (Duvenhage and Kröger 1996, Rooyen 2008). Hence, it is imperative to conduct researches on wind loading of ACS.

It is well-known that wind loading is one of the most important design loads of various buildings, especially for long-span bridges, long-span space structures, high-rise buildings, transmission towers and other special structures (Ke *et al.* 2016, Rodrigues *et al.* 2017, Edgar and Sordo 2017). Experimental and numerical researches on wind loads have been carried out extensively. However, there are a few works relevant to ACC, which mainly focus on the cooling performance of ACC. Gu *et al.* (2007) studied the recirculation of exhaust air at the ACC platform by wind tunnel testing, it was found that the wind speed, wind direction and height of the steel platform have significant effects on the recirculation. Furthermore, Gu *et al.* (2011) used a numerical simulation method to optimize the apron walls under the platform, and they found that the performance of direct air-cooling system is very sensitive to many environmental factors such as wind direction, topographic conditions and wind speed. Overall, the impact of strong wind on the system performance can be relieved by installing the apron walls.

As well-known, wind tunnel test method often plays an essential role on determining wind loads of new structures. Li *et al.* (2015) investigated the effects of non-uniformity morphological parameters of buildings on the drag coefficient through wind tunnel studies. It is well-known

∗Corresponding author, Ph.D. student
E-mail: xjdrenqianqian@163.com
[a] Professor
E-mail: yazhou_xhu@163.com
[b] Professor
E-mail: guoliangbai@126.com
[c] Ph.D.
E-mail: lihongxing@nwepdi.com

http://www.techno-press.com/journals/was&subpage=7 ISSN: 1226-6116 (Print), 1598-6225 (Online)

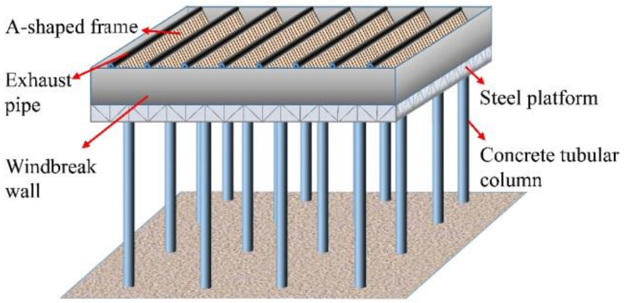

Fig. 1 Schematic of an air-cooling structure system

that the shape of buildings has a great influence on the wind pressure coefficient. Yang *et al.* (2016) studied the performance of a transmission tower through wind tunnel tests and computational fluid dynamics (CFD) simulations, some useful suggestions for calculating wind loads were reported for this kind of structures. Badri *et al.* (2015) presented an introduction to the available approaches of wind load calculations for high-rise buildings through the wind tunnel test. Although the seismic performance and design suggestions for ACS have been reported by Xu *et al.* (2015) and Du *et al.* (2017), there is few available work about wind loading of ACS in public.

In fact, the air-cooling structure is a flexible structure with irregular configuration, which is the cause of severely irregular distributions of vertical stiffness and mass. Apparently, code regulations of wind loading in the general design standards, e.g., GB 50009-2012 (2012), are not directly applicable to ACS. Hence, the specific parameter values for wind loads of ACS should be specially studied.

In this work, considering the comprehensiveness of the test results and universality of the application, two 1/150 scaled three-span models were designed and fabricated to conduct wind tunnel testing, corresponding to a rigid model and an aero-elastic model. The rigid model was used for testing the wind pressure distribution of the ACS, and the stiffness of which was higher than that of the aero-elastic model. The design and testing plan of the rigid model and aero-elastic model were firstly introduced in Section 2. Then, based on the experimental results of wind pressure of the rigid model and the wind-induced dynamic responses of the aero-elastic model, the design parameters of wind loads for ACS were determined in Section 3, which included the shape coefficients of “A” shaped frame and windbreak walls, the gust factor of the windbreak walls, and the wind vibration coefficient. The factors including wind direction angle and rotation of fan were taken into account in this section. Next, based on the computation method of wind load in Chinese load design standard, the parameters obtained in this paper provided a reference for wind-resistance design and engineering application of the air-cooled structure, which was introduced in Section 4. And some conclusions and suggestions were finally drawn in Section 5.

2. Wind tunnel testing setup and models

As mentioned previously, ACS exhibits special and complicated configurations, in which the lower part is a group of cylinder-shaped concrete columns, the middle part is the space truss, and the upper part is the A-shaped frame enclosed with rectangular windbreak walls. Compared to the sparsely arranged cylinder concrete columns in the lower part and hollow steel truss in the middle, wind loads acting on the rectangular windbreak walls and A-shaped frames in the upper, due to the larger windward area and higher wind speed, must play a major role on the wind-induced responses. Hence, in this study wind tunnel testing method was employed to investigate the wind-induced response and corresponding parameters of wind loads for the scaled ACS models.

2.1 Testing setup

The wind tunnel tests were conducted in an atmospheric boundary layer wind tunnel. The tunnel has a rectangular cross-section, containing a test section with 3.0 m (H) × 2.5 m (W) × 15.0 m (L). The wind speed ranges from 0 m/s to 53.0 m/s. Under steady conditions, the wind tunnel is capable of providing a uniform flow field, in which the turbulence intensity is less than 0.5%. There are two turntables in the wind tunnel test section. This experiment was conducted in the rear turntable with diameter of 2.0 m, and the distance between the center of the rear turntable and test section is 12.5 m. The reference height of the mean wind speed is 0.75 m. A photograph of the wind tunnel is shown in Fig. 7. The wind tunnel testing adopts automatic measurement and control systems. The signal collecting and analyzing system can synchronously record real-time data.

B type wind field was simulated in this test according to the design requirement of the prototype air-cooled structure. The surface roughness was realized by means of setting up steeples, cubic rough elements and toothed belts. Through continuously tuning, the target wind field was finally simulated according to the geometric scale ratio of 1/150. A Pitot tube and a thermal anemometer were used for measuring wind speed. The four-channel streamline hot-wire anemometer was employed for the adjustment and determination of wind field in atmospheric boundary layer, the measuring velocity and frequency response range of which were 0.02-300 m/s and 0-450 kHz, respectively, so that the mean wind speed, wind velocity profile, turbulence intensity and power spectrum of the wind tunnel were determined. The 256-channel electronic scanning pressure (ESP) measurement system was employed for measuring wind pressure, the pressure sensor range of which could support a column of water up to 254 mm high. The displacement measurement system was composed of the 64-channel data analysis and acquisition system, the laser displacement meter, accelerometer, PC and data processing software. The wind velocity profile, turbulence intensity profile and power spectrum of fluctuating wind generated in the wind tunnel are shown in Figs. 2 and 3, respectively. It is easy to find that the simulated results are consistent with the theoretical values. For the parameters in Figs. 2 and 3, U

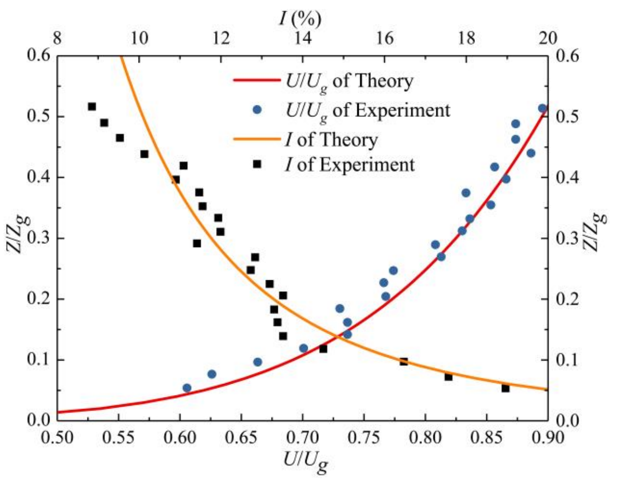

Fig. 2 The velocity and turbulence intensity profiles of B type wind field simulated by the wind tunnel

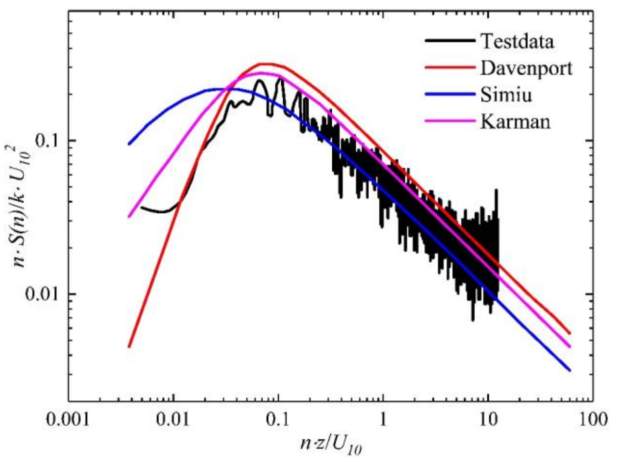

Fig. 3 Power spectrum of fluctuating winds simulated by the wind tunnel

is the mean wind speed (m/s) at the height Z (m); U_g is the reference wind velocity at the reference height Z_g; $S(n)$ is the power spectrum of fluctuating wind. In this study, $S(n)=0.26kU^2_{10}(1/(nx^{2/3})$, where $x=nz/U^2_{10}$, k is the coefficient of surface roughness, n is the gust frequency (Hz), U_{10} is the reference wind velocity (m/s) at height of 10 m. I is the turbulence intensity, which can be calculated by $I(z)=I_{10}\ (z/10)^{-\alpha}$. I_{10} is the nominal turbulence intensity at height of 10 m, which is 0.14 in this study.

2.2 Model design and manufacture

The height of the prototype ACS is 58.0 m and the maximum span is 25.4 m. The inside and outside diameters of cylinder-shaped concrete columns are 3.0 m and 3.8 m, respectively, and the height is 36.8 m. The maximum overhanging span of the steel truss is 14.5 m, the height is 7.4 m and the plane sizes of the truss are 106.5 m (L) × 92.4 m (W). The upper part is the A-shaped frame and exhaust pipe enclosed with rectangular windbreak walls, the heights of the A-shaped frame and windbreak walls are 9.4 m and 13.0 m, respectively. The overall structure is a steel-concrete hybrid structure system. According to the actual sizes of the wind tunnel test section, the geometric scale ratio of the models was chosen to be 1/150. The three-span rigid model and the aero-elastic model were then made according to the same scale ratio, the maximum length and width of the scaled model were 61.3 cm and 60.0 cm, respectively, and the overall height was 38.7 cm.

2.2.1 The rigid model

The rigid model needs to meet the similarity principle and requirements of strength and stiffness. According to the scale ratio, the fabricated rigid model is shown in Fig. 4. In order to ensure adequate stiffness of the testing model, the A-shaped frame and steel truss were made of ABS plastic, the tubular columns were made of organic glass. Fans of the scaled model were simulated by the computer CPU fans, the speed of which was 2500 rad/min. This test was conducted with a reference stream velocity of approximately 6.5 m/s, which could meet the actual wind speed at the location of the prototype structure after calculating based on the design standards. The fabrication process of the rigid model is shown in Figs. 5(a)-5(c). For each measured point, a scanning valve system was used to record pressure with a sampling frequency of 100 Hz and a sampling time of 9.6 s. In this test, the reference point for wind pressure was specified at a site between the left wall of the wind tunnel and turntable, with height of 1.2 m corresponding to actual height of 180 m in terms of the similarity law. The testing conditions were mainly determined by experimental factors including the wind incidence angle and rotation of fan. The incremental wind direction angle was 45°, there were eight wind direction angles in this work, as shown in Fig. 6(a).

Through reasonable layout of measuring sensors in the model, the wind pressures were measured under the different condition of wind incidence angle and rotation of fan, then the shape coefficient and gust factor were determined. For the convenience of identification and description, partitions of windbreak walls were identified with area A, B, C and D. Each area was equipped with pressure taps on the external and internal surfaces, with 29 taps on each side of area A, 60 taps on each surface of area B and D, and 27 taps on each side of area C, as shown in Fig. 6(a). The "A" shaped frames were divided into 16 areas from M1 to M16, and 30 measurement points were set in each area, as illustrated in Figs. 6(a) and 6(b).

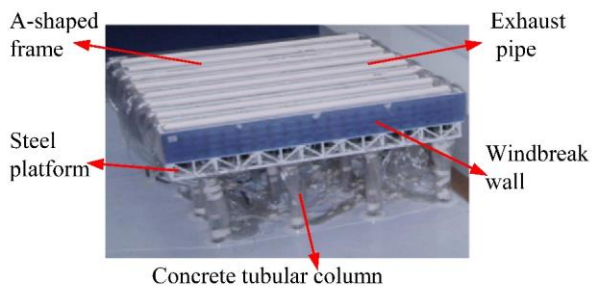

Fig. 4 Photo of the rigid model

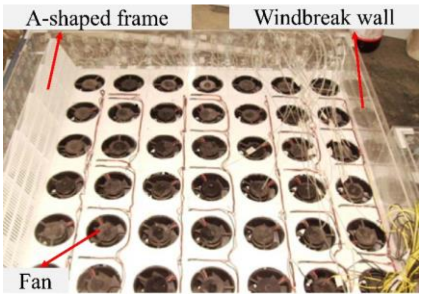

(a) Fans

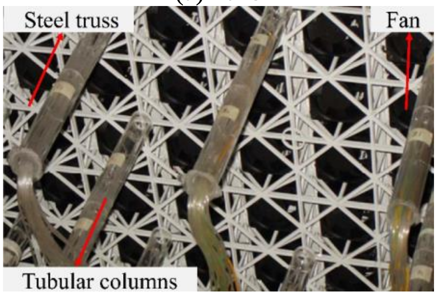

(b) Tubular columns

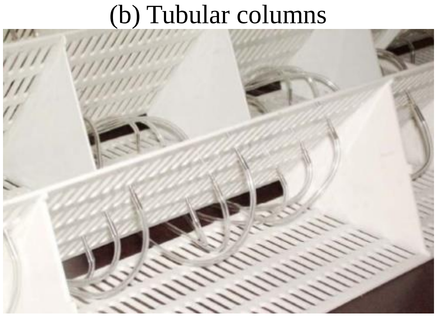

(c) A-shaped frame

Fig. 5 Photos of the fabrication process of (a) Fans (b) tubular columns (c) A-shaped frame

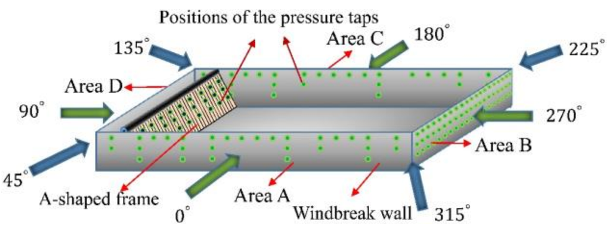

(a) Positions of pressure taps, and partition numbers of wind direction angles and windbreak walls

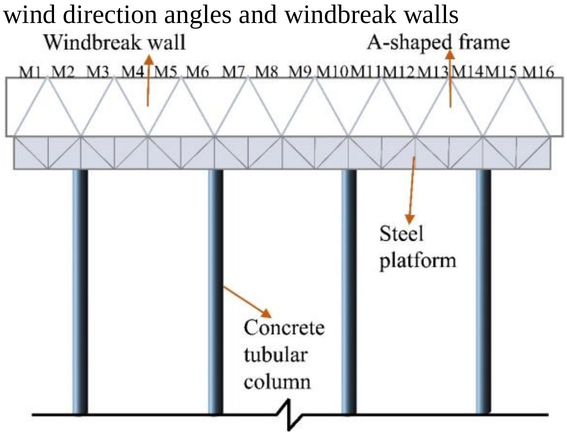

(b) Labels of “A” shaped frames

Fig. 6 Schematic of the rigid model

Fig. 7 Photo of the aero-elastic model

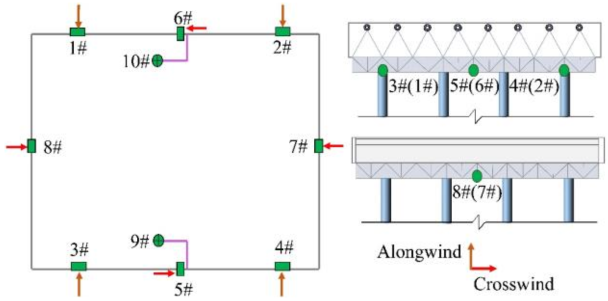

Fig. 8 Schematic view of the layout of the laser displacement meters and accelerometers

2.2.2 The aero-elastic model

The modal analysis of the finite element model of the prototype ACS was conducted to determine its natural frequencies and mode shapes. And the first three frequencies were 0.64 Hz, 0.68 Hz, and 0.73Hz, respectively, which were the basis for designing the aero-elastic model. According to the law of similarity, the scaled ratio of size was 1/150, the ratio of wind speed was 1/6 and the ratio of frequency ratio was 1/25. The columns of the aero-elastic model were simulated by steel bars with diameter of 6mm, the truss members were modeled by hollow square steel tubes of 3 mm×3 mm, and foams were around the column in order to meet the requirements of the windward area. As mentioned previously, fans of computer were used to simulate the disturbed effect by draught fans of ACC. And the windbreak walls and “A” shaped frames were made of organic glass. The real aero-elastic model is displayed in Fig. 7. Based on the finite element analysis of the prototype structure, the first three frequencies of the theoretical aero-elastic model were calculated in terms of the similarity law as 16.01 Hz, 17.45 Hz, and 18.23 Hz, respectively. And the experimental first three frequencies of the aero-elastic model were 16.02 Hz, 16.89 Hz, and 19.14 Hz, respectively, which indicated that the relative error between the prototype structure and the tested aero-elastic model was very small. It verified the design of the aero-elastic model.

The test wind speeds for the aero-elastic model ranged from 2.4 m/s to 10.0 m/s, the step length of which was 0.4 m/s from 2.4 m/s to 6.0 m/s, and 0.5 m/s from 6.0 m/s to 10.0 m/s. For all cases, data were sampled with a rate of 100 Hz for 41 s. Cases relevant to 6.0 m/s and 6.5 m/s were investigated especially in detail, which were close to the reference wind speed of the prototype structure.

Similar to the rigid model shown in Fig. 6(a), the incremental wind direction angle was also 45° in the wind tunnel test. In order to measure the along-wind and across-wind responses of the model, eight laser displacement meters and two accelerometers were arranged. The measurement points were just installed at the height of the steel truss, which was corresponding to 40.5 m high for the prototype structure. The laser displacement meters were installed at 1#~8# points, as shown in Fig. 8, among which the 1#~4# displacement meters were used for measuring the along-wind vibration response, the 5#~8# displacement meters were used for the across-wind vibration response, and the arrows indicated corresponding directions of the laser displacement meters. Besides, the 9#~10# accelerometers were used for measuring the acceleration response. The layout of the sensors is illustrated in Fig. 8.

3. Experimental results and analysis

3.1 Computation formula of wind loads

Based on the computation method of wind load in Chinese load design standard (GB 50009-2012, 2012), the main design parameters of wind loads for ACS need to be determined through the wind tunnel tests, including the shape coefficient (μ_s), the coefficient of wind pressure which varies with height (μ_z), and the wind vibration coefficient (β_z). The wind load in Chinese load design standard could be computed by

$$W_k = \beta_z \mu_s \mu_z W_0 \tag{1}$$

where W_0 is the basic wind pressure (kN/m^2), which is regulated in GB 50009-2012 for different regions. μ_z is the coefficient of wind pressure which varies with height, and it can be calculated for B type wind filed with $\mu_z = 1.0(z/10)^{0.3}$. z is the height from the ground (m). Moreover, if windbreak walls are treated as the enclosure component with larger stiffness, the gust factor (β_{gz}) should be employed.

3.1.1 Shape coefficient μ_s and gust factor β_{gz}

According to the experimental results of wind pressure of the rigid model, the design parameters of wind loads for ACS, including the gust factor and load shape coefficient, could be calculated. Based on wind pressure at the reference point in a wind tunnel, a dimensionless wind pressure coefficient C_{pr} could be defined with Eq. (2) as following,

$$C_{pr} = \frac{p - p_{r\infty}}{p_{r0} - p_{r\infty}} \tag{2}$$

where p is the dimensional wind pressure measured in the wind tunnel. p_{r0} and $p_{r\infty}$ are the total pressures and static pressures at the reference point, respectively.

The wind pressure coefficient C_{pr} is related to the kind of the simulated wind filed, and B type wind field is specified in this test. In order to apply the experimental results to other wind fields, it is necessary to transfer the wind pressure at the reference point in the wind tunnel to corresponding gradient wind pressure, which is independent of ground topography.

For the wind profile specified with the law of power function $U=U_g(Z/Z_g)^{\alpha}$, the dimensionless wind pressure coefficient C_p with the gradient wind pressure as reference could be expressed as Eq. (3).

$$C_p = (Z_r / Z_g)^{2\alpha} C_{pr} \tag{3}$$

where Z_g is the height of the gradient wind; α is a power exponent that reflects the roughness of regulated ground topography; Z_r is the actual height which is calculated according to the scale ratio at the height of the reference point. With α=0.15, Z_g =350 m and Z_r =180 m in accordance with GB 50009-2012 (2012), one have C_p=0.8191C_{pr}. Hereafter, $C_{p\text{mean}}$ denotes the wind pressure coefficient of mean wind, and $C_{p\text{rms}}$ represents the RMS pressure coefficient of fluctuating wind, which could be calculated by statistical analysis of the experimental wind pressure.

Moreover, the maximum wind pressure coefficients $C_{p\max}$ and the minimum wind pressure coefficients $C_{p\min}$ could be calculated by following equations

$$\begin{aligned} C_{p\max} &= C_{p\text{mean}} + gC_{p\text{rms}} \\ C_{p\min} &= C_{p\text{mean}} - gC_{p\text{rms}} \end{aligned} \tag{4}$$

where g is the peak factor, which is 2.5 in this study according to the Chinese load code. Considering that $C_{p\text{mean}}$ is defined with the gradient wind pressure as reference, the local shape coefficient at each measured point can be computed as follows

$$\mu_{si} = (\frac{Z_g}{Z_r})^{2\alpha} C_{p\text{mean}} = 1.22 C_{p\text{mean}} \tag{5}$$

The overall shape coefficient for each partition is the weighted average of the local shape coefficients of all the measurement points in the partition, which can be expressed as Eq. (6).

$$\mu_s = \sum \mu_{si} A_i / \sum A_i \tag{6}$$

where A_i is the control area (m^2) of the ith measurement point in a partition. $\sum A_i$ is the total area (m^2) of all the measurement points in the partition under consideration.

Besides, based on Eq. (4), the local gust factor could be defined as follows

$$\beta_{gz,i} = \frac{C_{p\max}}{C_{p\text{mean}}} = 1 \pm g\frac{C_{p\text{rms}}}{C_{p\text{mean}}} \tag{7}$$

Similarly, the overall gust factor can be calculated by Eq. (8).

$$\beta_{gz} = \frac{\sum \beta_{gz,i} A_i}{\sum A_i} \tag{8}$$

3.1.2 Wind vibration coefficient β_z

Wind load is often decomposed into the mean component and fluctuating component. Wind vibration coefficient is defined as the ratio of the structural response caused by the total wind load to that of the mean component. In this study, the wind vibration coefficient based on structural displacement can be expressed as the ratio of the total displacement to the static displacement due to mean wind. Moreover, the total displacement is the sum of the static displacement and the dynamic displacement induced by the fluctuating component.

Through the aero-elastic model, the static displacement D_{si} of the measured points was obtained by averaging the time history of experimental displacements, while the dynamic displacement was determined by the peak factor g and the displacement standard deviation σ_i. So, the wind vibration coefficient can be calculated as following

$$\beta_{z,i} = 1 + \frac{g\sigma_i}{D_{si}} \tag{9}$$

As shown in Fig. 8, the 1#, 2#, 3# and 4# measured points were arranged symmetrically, and the 5#, 6#, 7#, and 8# measured points were also arranged symmetrically. The along-wind direction of each measured point varies with the wind direction angle, as shown in Fig. 6(a) and Fig. 8. The 1# and 2# measured points were in the along-wind direction when the wind direction angle was 0°, the 3# and 4# measured points were in the along-wind direction when the wind direction angle was 180°, and the 5#, 6#, 7#, and 8# measured points were in the along-wind direction when the wind direction angle was 270°. Thus, the wind vibration coefficient of the whole model in the along-wind direction can be calculated by averaging the wind vibration coefficients of those in two directions as Eq. (10).

$$\begin{aligned} \beta_z &= \frac{\beta_{1\#}^{0^{\circ}} + \beta_{2\#}^{0^{\circ}} + \beta_{3\#}^{180^{\circ}} + \beta_{4\#}^{180^{\circ}}}{4} \\ \beta_z &= \frac{\beta_{5\#}^{270^{\circ}} + \beta_{6\#}^{270^{\circ}} + \beta_{7\#}^{270^{\circ}} + \beta_{8\#}^{270^{\circ}}}{4} \end{aligned} \tag{10}$$

where the subscript denotes the number of measured point, and the superscript represents the corresponding wind direction angle.

The measured points of the tested aero-elastic model were just arranged at height of the steel truss of the testing model, which corresponded to 40.5 m of the prototype structure. However, in practice wind vibration coefficients at different heights should be given in order to compute the wind load. The formula of wind vibration coefficients in the standard is expressed by Eqs. (11) and (12) in Section 3.2.3.

3.2 Experimental parameters of wind load

3.2.1 The shape coefficient

Based on the experimental wind pressure of the rigid model, the shape coefficients of “A” shaped frame and windbreak walls could be calculated according to Eq. (6). It was found that the rotation of fans had a slight effect on the wind pressure distribution of the model, which reduced the wind pressure and its corresponding values of the global shape coefficients of the “A” shaped frame and windbreak walls. Moreover, the shape coefficients of “A” shaped frame with running fans were all less than those without running fans. It meant that the change of the wind field owing to running fans weakened the wind pressure distribution on the model. For instance, the influence of running fans on the shape coefficient of M16 of the “A” shaped frame is illustrated in Fig. 9.

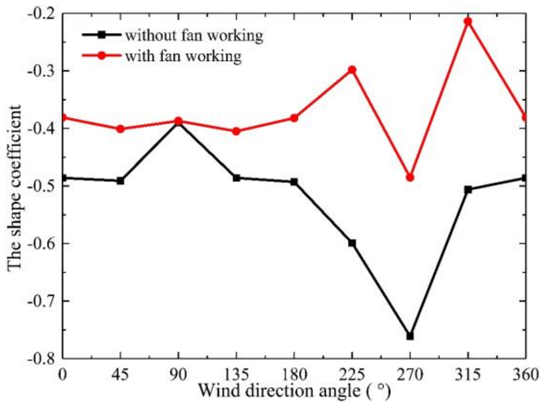

Fig. 9 The influence of running fans on the shape coefficient of M16 on the “A” shaped frame

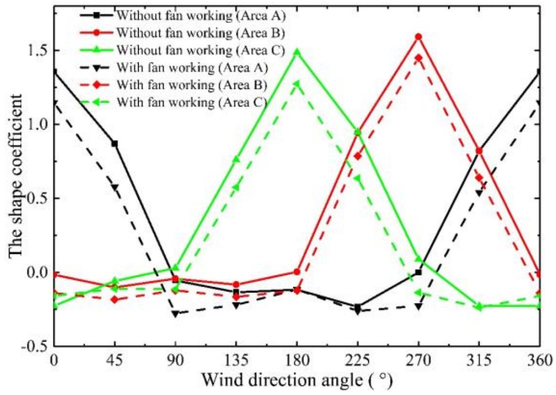

Fig. 10 The influence of running fans on the windbreak walls

Likewise, for the windbreak walls the shape coefficients with running fans were also smaller than those without running fans, as shown in Fig. 10. For the sake of conservation, the shape coefficients without running fans were taken as design values of ACS.

Taking the symmetry into account, the overall shape coefficient of each partition could be determined according to Eq. (6). The overall shape coefficients of the rigid model under different wind direction angles are listed in Table 1.

As shown in Table 1, the wind direction angle has great influence on the distribution of wind pressure. For the windbreak walls, i.e. area A, B, C and D, the wind loads on the windward sides are pressure, which would gradually become suction as the change of wind direction angles, corresponding to the leeward or sideward cases. Besides, the wind loads of windbreak walls on the leeward side are always suction, e.g. area C with wind direction angle of 0° and area A with wind direction angle of 180°. Moreover, it is noteworthy that wind loads of “A” shaped frames are all suction due to the shielding effect of windbreak walls, and the overall shape coefficients of each “A” shaped frame show little variation.

Additionally, the local shape coefficient distribution of area A is shown in Fig. 11, which reflects the detailed distribution of wind loads in accordance to wind direction angle of 0°. It can be found that the wind pressure on the windward sides are positive, and the wind pressure coefficients of the lower arts are larger than those of the upper part, which mainly results from the bottom edge of the windbreak wall connected with the steel truss, while the top edge approximately being free.

Due to the shielding effects of windbreak walls, the values of the "A" shaped frame are all negative. The overall shape coefficients of each "A" shaped frame vary little. When the inflow direction is 0°, the local shape coefficient distribution of "A" shaped frame M16 is shown in Fig. 12. It shows that the pressure values are all negative, which will gradually decrease along the wind direction.

Table 1 The overall shape coefficients μ_s of "A" shaped frame and windbreak walls of the rigid model

Area	Wind direction angle θ							
	0°	45°	90°	135°	180°	225°	270°	315°
M1	-0.49	-0.51	-0.76	-0.60	-0.49	-0.49	-0.39	-0.49
M2	-0.46	-0.47	-0.70	-0.52	-0.51	-0.52	-0.40	-0.46
M3	-0.51	-0.51	-0.75	-0.61	-0.46	-0.49	-0.39	-0.48
M4	-0.48	-0.44	-0.61	-0.47	-0.52	-0.49	-0.40	-0.43
M5	-0.52	-0.45	-0.69	-0.53	-0.47	-0.48	-0.39	-0.46
M6	-0.47	-0.41	-0.52	-0.46	-0.53	-0.49	-0.44	-0.40
M7	-0.52	-0.42	-0.58	-0.50	-0.47	-0.46	-0.41	-0.44
M8	-0.47	-0.42	-0.45	-0.44	-0.52	-0.48	-0.50	-0.41
M9	-0.52	-0.41	-0.50	-0.48	-0.47	-0.44	-0.45	-0.42
M10	-0.47	-0.44	-0.41	-0.46	-0.52	-0.50	-0.58	-0.42
M11	-0.53	-0.40	-0.44	-0.49	-0.47	-0.46	-0.52	-0.41
M12	-0.47	-0.46	-0.39	-0.48	-0.52	-0.53	-0.69	-0.45
M13	-0.52	-0.43	-0.40	-0.49	-0.48	-0.47	-0.61	-0.44
M14	-0.46	-0.48	-0.39	-0.49	-0.51	-0.61	-0.75	-0.51
M15	-0.51	-0.46	-0.40	-0.52	-0.46	-0.52	-0.70	-0.47
M16	-0.49	-0.49	-0.39	-0.49	-0.49	-0.60	-0.76	-0.51
A	1.36	0.81	-0.05	-0.13	-0.12	-0.23	0.00	0.82
B	-0.02	-0.10	-0.04	-0.08	0.00	0.94	1.59	0.82
C	-0.23	-0.06	0.03	0.76	1.49	0.95	0.09	-0.23
D	0.00	0.82	1.59	0.94	-0.02	-0.08	-0.04	-0.10

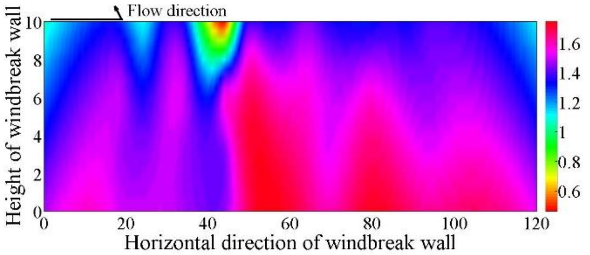

Fig. 11 Cloud diagram of the local shape coefficient on area A of the windbreak walls when θ=0°

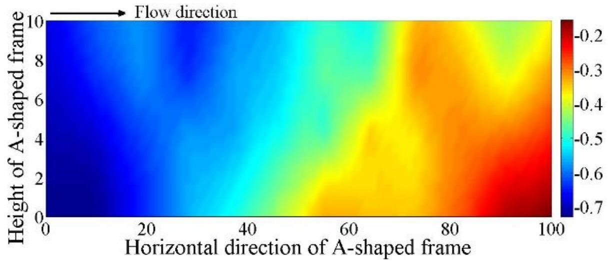

Fig. 12 Cloud diagram of local shape coefficients of "A" shaped frame M16 when θ=0°

3.2.2 The gust factor

According to the Chinese load code (GB 50009-2012, 2012), for maintaining components with adequate rigidness, the wind loads should be calculated with the gust factor without consideration of the structural vibration. In terms of the experimental results of the rigid model, the gust factor of windbreak walls was calculated according to Eq. (8). The results with and without running fans are listed in Tables 2 and 3.

As shown in Tables 2 and 3, the disturbance caused by fans has little influence on the gust factor on the windward side, but there is a significant increase on the leeward side. The reason may be interpreted as the fluctuating components being dominant in the cases of the leeward and crosswind. Meanwhile, wind direction angles have considerable influence on the gust factor of the windbreak walls. The gust factors on the windward sides are generally around 1.5, e.g., area A with wind direction angle of 0° and area C with wind direction angle of 180°. The values on the leeward side and crosswind side are relatively large, but the global wind pressures are still small after considering the impact of fluctuating pressure.

3.2.3 The wind vibration coefficient

The structural along-wind direction responses are major concerns for engineering design. Accordingly, it is the fundamental purpose in this study to determine the wind vibration coefficient in the along-wind direction for ACS.
Based on the analysis of the experimental data and definition of wind vibration coefficient, the measured results were employed to determine the wind vibration coefficients when wind speeds were from 22.6 m/s to 46.2 m/s. The wind speeds listed in the table are the actual wind speeds in terms of the similarity law.

Table 2 Gust factor β_{gz} under different wind direction angles with consideration of running fans

Area	Wind direction angle θ							
	0°	45°	90°	135°	180°	225°	270°	315°
A	1.59	1.79	1.90	2.01	2.46	1.74	1.73	1.74
B	2.92	2.07	1.84	1.99	3.15	1.59	1.54	1.70
C	2.59	2.37	2.78	1.77	1.55	1.73	3.40	2.03

Table 3 Gust factor β_{gz} under different wind direction angles without consideration of running fans

Area	Wind direction angle θ							
	0°	45°	90°	135°	180°	225°	270°	315°
A	1.53	1.53	3.11	2.93	3.86	2.18	4.69	1.54
B	4.72	2.57	2.44	2.99	3.89	1.50	1.49	1.61
C	2.99	4.21	3.62	1.60	1.60	1.55	3.32	2.23

Table 4 The wind vibration coefficient of the 1#~4# measured points

Test wind speed (m/s)	Wind vibration coefficient β_z				
	1#0°	2#0°	3#180°	4#180°	Mean
22.6	1.90	1.67	1.99	1.85	1.85
30.8	1.63	1.21	2.48	1.75	1.77
33.4	1.73	1.35	2.50	1.67	1.81
38.5	1.60	1.31	2.24	1.56	1.68
46.2	1.54	1.41	2.47	1.50	1.73

Table 5 The wind vibration coefficient of the 5#~8# measured points

Test wind speed (m/s)	Wind vibration coefficient β_z			
	5#270°	7#270°	8#270°	Mean
22.6	1.32	1.41	1.80	1.51
30.8	2.33	1.25	1.76	1.78
33.4	2.22	1.24	1.68	1.71
38.5	1.76	1.24	1.65	1.55
46.2	2.00	1.24	1.63	1.62

For convenience to read, the wind vibration coefficients are also presented for different wind speeds in Tables 4-5. As the locations of the measured points are different and the flow field is complex, the wind vibration coefficients will be very sensitive with the change of wind direction angle. Subsequently, the averaged values of vibration coefficients would be calculated according to Eq. (10), which can be regarded as the wind vibration coefficient of the structure center in two directions.

Due to the limitation of the test conditions, the measured points of the aero-elastic model were just arranged at height of the steel truss of the testing model. Nevertheless, in practice wind vibration coefficients at different heights should be given in order to compute the wind load. As specified in the Chinese load code, the formula of wind vibration coefficients is expressed as following

$$\begin{aligned} &\beta_z(z) = 1 + 2gI_{10}B_z\sqrt{1+R^2} \\ &B_z = kH^{\alpha_1}\rho_x\rho_z\frac{\phi_1(z)}{\mu_z} \\ &R = \sqrt{\frac{\pi}{6\zeta_1}\frac{x_1^2}{(1+x_1^2)^{4/3}}} \\ &x_1 = \frac{30f_1}{\sqrt{k_wW_0}} \end{aligned} \tag{11}$$

where g is peak factor, the value is 2.5 according to the Chinese load code. I_{10} is the nominal turbulence intensity at height of 10 m, which is 0.14 in this study. R is the resonance component factor of fluctuating wind load, the proposed value in this study is 1.159. B_Z is the background component factor of wind loads. H is the total height of structure, which is 58.0 m in this paper. ρ_x and ρ_z are correlation coefficients in horizontal and vertical directions, the calculated values according to the experimental results are 0.742 and 0.787, respectively. μ_z is the coefficient of wind pressure which varies with height, for B type wind filed it can be calculated with μ_z=1.0$(z/10)^{0.3}$. z is the height from the ground (m). k and α_1 are the factors which take values of 0.910 and 0.218 according to the Chinese load code. $\phi_1(z)$ is the modal coefficient, which would be specified in terms of the first-order vibration shape. ζ_1 is damping ratio, which is 0.04 in this paper. f_1 is the first natural frequency, the value is 0.64 Hz here. W_0 is the fundamental wind pressure, which is 0.4 kN/m^2 in this study. k_w is the correction factor of surface roughness, which is 1.0 according to the load code.

Based on the finite element simulation of the prototype structure and the dynamic testing results of the tested aero-elastic model, the modal coefficient of ACS can be computed by the following fitted function

$$\phi_1(z) = -2.5292(z/H)^3 + 3.5004(z/H)^2 + 0.0204(z/H) \tag{12}$$

The measured points of the aero-elastic model were just arranged at height of the steel truss of the testing model, which corresponded to 40.5 m of the prototype structure. Therefore, the parameter z is 40.5 m. Using the fitting function of the modal coefficient, the predicted wind vibration coefficient at the height of the measured points is 1.78, which shows a reasonable agreement with the mean values of wind tunnel testing in Tables 4 and 5. Moreover, the wind vibration coefficients at other heights can be calculated by Eqs. (11) and (12).

4. Calaulation of wind loads for air-cooling structures

Hereto, the main design parameters of wind loads for ACS in accordance with Chinese standard (GB 50009-2012, 2012) have been determined according to the wind tunnel testing results. The experimental results and calculation formulas of shape coefficient and wind vibration coefficient have been presented previously. "A" shaped frame and windbreak walls of ACS are considered in the whole structure due to their firmly connection with main structure in this study, the standard wind load could be computed by Eq. (1). Due to the particularity of the air-cooling structure, the parameter values are different from other structures such as the saw-tooth roofs described in the specification. For convenience to read, the proposed values of these parameters are summarized as below.

The shape coefficients μ_s of "A" shaped frame along the windward direction (θ=0°) and across wind direction (θ=90°) are shown in Figs. 13 and 14, respectively. The values of the "A" shaped frame are all negative due to the shielding effects of windbreak walls. When the wind direction is parallel to the "A" shaped frame (θ=0°), the overall shape coefficients of each "A" shaped frame vary little. When the wind direction is perpendicular to the "A" shaped frame (θ=90°), the pressure values are all negative, which will gradually decrease along the wind direction. The values of other wind conditions can refer to Table 1.

As shown in Table 1, the wind loads of windbreak walls are pressure on the windward side, and are always suction on the leeward side, e.g., area C with wind direction angle of 0° and area A with wind direction angle of 180°.

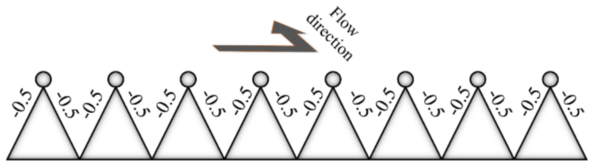

Fig. 13 Global shape coefficient of "A" shaped frame μ_s when θ=0°

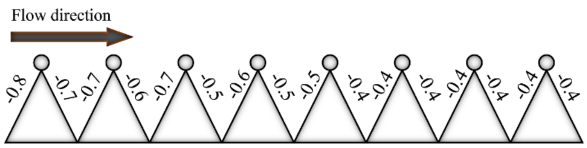

Fig. 14 Global shape coefficient of "A" shaped frame μ_s when θ=90°

Table 6 The shape coefficient μ_s of windbreak walls

Area	Wind direction angle θ		
	0°	180°	270°
Windward side	1.4	1.5	1.6
Leeward side	-0.2	-0.1	0.0
Crosswind side	0.0	0.0	0.1

Table 7 The wind vibration coefficients β_z of the ACS model

Normalized height (*z/H*)	μ_z	$\phi_1(z)$	β_z
0.1	1.00	0.04	1.06
0.2	1.05	0.12	1.16
0.3	1.18	0.25	1.29
0.4	1.29	0.41	1.44
0.5	1.38	0.57	1.57
0.6	1.45	0.73	1.69
0.7	1.52	0.86	1.78
0.8	1.58	0.96	1.84
0.9	1.64	1.00	1.84
1	1.69	1.00	1.81

In order to be consistent with the specification (GB 50009-2012, 2012), the shape coefficients of windbreak walls are shown in Table 6, including windward side, leeward side and crosswind side.

Through Eqs. (11) and (12), the predicted wind vibration coefficient at the height of the measured points shows a reasonable agreement with the mean values of wind tunnel experiments. Therefore, the wind vibration coefficients β_z at different heights can be calculated in order to keep consistent with the standard, as listed in Table 7. The coefficients of wind pressure varying with the height μ_z for B type field are also listed in Table 7.

Moreover, if windbreak walls are treated as the enclosure structure with larger stiffness, the gust factor should be employed. The experimental gust factors of windbreak walls for ACS are presented in Tables 2 and 3.

5. Conclusions

In order to determine the wind loads of ACS, wind tunnel testing of 1/150 scaled models were designed and conducted. The influence factors including wind direction angle and rotation of fan were taken into account. The wind tunnel test of the three-span rigid model was firstly carried out. Based on the experimental results of wind pressure, the overall shape coefficients of the "A" shaped frame and windbreak walls, the gust factor of the windbreak walls were obtained. Then, tests of the aero-elastic model were carried out in order to study the wind-induced vibration responses, and the wind vibration coefficients of the ACS model were obtained. Finally, based on the computation method of wind load in Chinese load design standard, the design parameters of ACS were presented, which provide reference for wind-resistance design and engineering application to this kind of structure.

The main conclusions are summarized as follows:

- The presence of running fans would slightly reduce the wind pressure of the "A" shaped frame and windbreak walls, while it has less influence on the wind vibration coefficients. Therefore, it has been neglected in the proposed design method for safety of the air-cooled structure.
- Due to the shielding effects of windbreak walls, the wind pressures of the "A" shaped frame are all suction. When the inflow direction is parallel with the direction of the "A" shaped frame (wind direction angle θ=0°), the shape coefficients of each "A" shaped frame vary little. When the wind direction is perpendicular to the "A" shaped frame (θ=90°), the pressure values are all negative, which will gradually decrease along the wind direction.
- For the windbreak walls, the wind loads in the windward direction are positive pressure, and the values of shape coefficients in this direction are larger than those in the other directions.
- Based on the dynamic testing of the aero-elastic model, the first order vibration shape was fitted to calculate the wind vibration coefficient.

- In this study, focus are mainly put on the wind loads of “A” shaped frame and windbreak walls, while wind loading of the tubular concrete columns could be determined with the published researches and design methods in the codes.
- Based on the proposed parameters of the shape coefficient, gust factor and wind vibration coefficient, the wind loads can be calculated for the air-cooled structure.

Acknowledgments

The support of the National Natural Science Foundation of China (Grant No. 51578444) and Program for Innovative Research Team in University of Ministry of Education of China (Grant No. IRT_17R84) is greatly acknowledged.

References

Badri, A.A., Hussein, M.M. and Attia, W.A. (2015), “Study of wind tunnel test results of high-rise buildings compared to different design codes”, *Wind Struct.*, **20**(5), 623-642.

Butler, C. and Grimes, R. (2014), “The effect of wind on the optimal design and performance of a modular air-cooled condenser for a concentrated solar power plant”, *Energy*, **68**, 886-895.

Chen, L., Yang, L.J., Du, X.Z. and Yang, Y.P. (2016), “A novel layout of air-cooled condensers to improve thermo-flow performances”, *Appl. Energy.*, **165**, 244-259.

Duvenhage, K. and Kröger, D.G. (1996), “The influence of wind on the performance of forced draught air-cooled heat exchangers”, *J. Wind Eng. Ind. Aerod.*, **62**(2-3), 259-277.

Du, N.J., Bai, G.L., Xu, Y.Z. and Qin, C.G. (2017), “Experimental and numerical researches on the seismic behavior of tubular reinforced concrete columns of air-cooling structures”, *Int. J. Concr. Struct. Mater.*, **11**(3), 459-475.

Edgar, T.H. and Sordo, E. (2017), “Structural behaviour of lattice transmission towers subjected to wind load”, *Struct. Infrastruct. Eng.*, **13**(11), 1462-1475.

GB 50009-2012 (2012), Load code for the design of building structures, China Architecture and Building Press; Beijing, China.

Gu, H.F., Qiu, F.Q. and Wang, H.J. (2011), “Structure optimization of an air-cooling system platform at a large power plant”, *Heat Transf. Eng.*, **32**(11-12), 1069-1074.

Gu, Z.F., Chen, X.R. and William, L. (2007), “Wind tunnel simulation of exhaust recirculation in an air-cooling system at a large power plant”, *Int. J. Thermal Sci.*, **46**(3), 308-317.

He, W.F., Dai, Y.P., Wang, J.F., Li, M.Q. and Ma, Q.Z. (2013), “Performance prediction of an air-cooled steam condenser using UDF method”, *Appl. Therm. Eng.*, **50**(1), 1339-1350.

Ke, S.T., Wang, H. and Ge, Y.J. (2016), “Wind load effects and equivalent static wind loads of three-tower connected tall buildings based on wind tunnel tests”, *Struct. Eng. Mech.*, **58**(6), 967-988.

Li, B., Liu, J. and Gao, J.M. (2015), “Surface wind pressure tests on buildings with various non-uniformity morphological parameters”, *J. Wind Eng. Ind. Aerod.*, **137**, 14-24.

Li, X.E., Wang, N.L., Wang L.G., Yang, Y.P. and Maréchal, F. (2018), “Identification of optimal operating strategy of direct air-cooling condenser for Rankine cycle based power plants”, *Appl. Energy*, **209**, 153-166.

Maniscalco, N. (2014), “Design and performance characterization of high power density air-cooled compact condenser heat exchangers”, Ph.D. Dissertation, University of Illinois at Urbana-Champaign, Urbana, Illinois.

Moore, J., Grimes, R., Walsh, E. and O’Donovana, A. (2014). “Modelling the thermodynamic performance of a concentrated solar power plant with a novel modular air-cooled condenser.” *Energy*, **69**, 378-391.

Owen, M.T.F. and Kröger, D.G. (2011), “An investigation of air-cooled steam condenser performance under windy conditions using computational fluid dynamics”, *J. Eng. Gas Turbine Power.*, **133**(6), 831-844.

Rodrigues, A.M., Tomé, A. and Gomes, M.G. (2017), “Computational study of the wind load on a free-form complex thin shell structure”, *Wind Struct.*, **25**(2), 177-193.

Rooyen, J.A.V. (2008), “Performance trends of an air-cooled steam condenser under windy conditions”, *J. Eng. Gas Turbine Power.*, **130**(2), 277-285.

Xu, Y.Z., Bai G.L. and Zhu, J.N. (2015), “Pseudo-dynamic test and numerical simulation of a large direct air-cooling structure”, *Struct. Des. Tall Spec. Build.*, **24**(4), 280-299.

Yang, F.L., Dang, H.X., Niu, H.W., Zhang, H.J. and Zhu, B.R. (2016), “Wind tunnel tests on wind loads acting on an angled steel triangular transmission tower”, *J. Wind Eng. Ind. Aerod.*, **156**, 93-103.

Yang, L.J., Wang, M.H., Du, X.Z. and Yang, Y.P. (2012), “Trapezoidal array of air-cooled condensers to restrain the adverse impacts of ambient winds in a power plant”, *Appl. Energy*, **99**(6), 402-413.

AD